Fluorescent Antimicrobial Peptides Based on Nile Red: Effect of Conjugation Site and Chemistry on Wash-free Staining of Bacteria

Lucille Weiss,[a] Antoine Mirloup,[a] Léa Blondé,[b] Hanna Manko,[c] Jean Peluso,[b] Dominique Bonnet,[a] Dmytro Dziuba[c]#* and Julie Karpenko[a] #*

[a] Laboratoire d'Innovation Thérapeutique, Faculté de Pharmacie,
UMR 7200 CNRS/Université de Strasbourg, Institut du Médicament de Strasbourg,
F-67000 Strasbourg, France
e-mail: julie.karpenko@unistra.fr

[b] Plate-forme eBioCyt – UPS 1401, Faculté de Pharmacie,
Université de Strasbourg,
F-67000 Strasbourg, France

[c] Laboratoire de Bioimagerie et Pathologies, Faculté de Pharmacie,
UMR 7021 CNRS/Université de Strasbourg,
F-67000 Strasbourg, France
e-mail: dmytro.dziuba@unistra.fr

Abstract: Fluorescent probes for bacterial detection can be obtained by conjugating antimicrobial peptides with fluorescent dyes. However, little is known about the effect of the conjugation site and linker chemistry on staining efficiency. We synthesized three conjugates of the antimicrobial peptide ubiquicidin with the environmentally sensitive fluorophore Nile Red that differed by the attachment site and the chemical composition of the linker. We showed that incorporating fluorophore as a minimalistic non-natural amino acid resulted in a superior probe compared with the typically used bioconjugation approaches. The new peptide-based probe named **UNR-1** displayed red fluorescence and enabled robust wash-free staining of Gram-positive and Gram-negative bacteria. The probe exhibited selectivity over mammalian cells and enabled rapid fluorescence detection of bacteria by fluorescence microscopy and flow cytometry in an add-and-read format. Our results may foster the development of next-generation fluorescent AMPs for clinical laboratory diagnostics and medical imaging.

TOC:

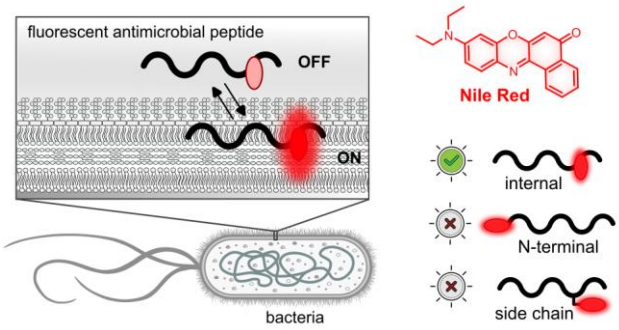

The worldwide spread of antibiotic-resistant bacteria poses a global threat to human health which must be addressed at multiple levels.[1–3] While developing new antimicrobials is resource-intensive and slow, new sensors and assays are required for fast and sensitive detection of bacteria in biological samples as an essential strategy for preventing and managing bacterial infections. Such sensors and assays would be of great practical utility in clinical laboratory diagnostics, fundamental biomedical research on host-pathogen interactions, environmental and quality control testing, and other applications. Ultimately, such sensors could moderate the overuse of antibiotics and alleviate the spread of antibiotic resistance.[4–11] Biosensing platforms based on fluorescence readout offer distinct advantages owing to the possibility for rapid analysis, high sensitivity, facile multiplexing, and compatibility with live cells and tissues. In addition, fluorescence analysis can be performed using various instruments, including portable devices for point-of-care diagnostics. Given that, bacteria-specific fluorescent molecular probes have received substantial attention as prospective bioanalytical tools for fundamental research and clinical diagnostics and imaging.[12–17]

A key advantage offered by the technology of fluorescent molecular probes is the possibility of combining desired optical properties with high target selectivity, high signal-to-noise ratios, and low detection limit by tailoring the molecular architecture of the probe. In this context, fluorogenicity refers to the ability of a probe to exhibit enhanced fluorescence upon interaction with the target as compared with the free probe in solution.[18–20] Rationally designed fluorogenic molecular probes are well suited for detecting low-abundance targets with high signal-to-noise ratios in biological samples.[21–23] Ideally, the assay should be performed with minimal sample processing in an “add-and-read” format.

In the field of bacterial pathogen detection, fluorescent and especially fluorogenic probes hold great promise compared to conventional microbiological assays.[13–16,24] The conventional assays based on microbial culture or nucleic acid detection techniques are indirect, time-consuming, and labor-intensive.[25] Contrary to that, bacteria-specific fluorescent probes are designed for direct staining of bacteria in the sample, enabling fast and sensitive detection of pathogens in complex media. Fluorescent probes could shorten the analysis time and increase the throughputness and cost-effectiveness of bacteria-detection assays.

Several pathogen-specific fluorescence labeling methods have been devised aiming at distinct phenotypic features of the bacterial cell.[26,27] A major group is represented by engineered fluorescent analogs of natural molecular building blocks that can be metabolically incorporated into the bacterial biopolymers and therefore render the exposed cells fluorescent.[28] The most prominent examples are synthetic analogs of sugars and D-amino acids.[29–31] Furthermore, fluorogenic substrates for bacteria-specific enzymes can generate a fluorescence response in the presence of bacteria.[32] Alternatively, fluorescent indicators based on small organic dyes that specifically stain bacteria have been designed.[24,33–36] Finally, bacteria-targeting fluorescent probes have been constructed by conjugating a fluorescence emitter with bacteria-targeting recognition units, such as antibiotics,[37] antibodies,[38,39] aptamers,[40] and cationic antimicrobial peptides (AMPs).[41] The latter ones hold great promise for the development of bacteria-targeting biosensors.[42–44] The use of AMPs as bacteria-recognizing units offers the following advantages. First, tens of thousands of AMPs with distinct selectivity profiles toward different types of bacteria have been documented,[45] enabling data-driven selection of an appropriate molecular vector. Second, the binding affinity, selectivity, and stability of the vector can be tuned by chemical modifications of the peptide. In general, recognition units based on AMPs are more robust and amenable to chemical modifications compared with antibodies and aptamers. Third, many AMPs of practical interest can be synthesized using solid-phase peptide synthesis (SPPS) and then conjugated to a reporter group using appropriate bioconjugation methods. Combining the broad range of available biocompatible fluorophores gives researchers a great degree of flexibility in designing peptide-based fluorescence staining reagents. Because of these factors, AMP-derived fluorescent probes have been intensively used for sensing and imaging of bacterial infections.[46–50] At the same time, the existing fluorescent AMPs display several limitations that need to be addressed. For instance, some fluorophores used in AMP-based reporters exhibit “always-on” fluorescence. Such probes suffer from the non-specific background signal and thus require additional washing steps to remove the unbound fraction from the sample. Another group of AMP-based probes exhibits a fluorogenic behavior but emits in the green region of spectra.[46] Such optical properties limit the range of applications because of the autofluorescence of live cells and tissues. Very few fluorogenic AMP-based probes operating in the red spectral region have been described.[47] Besides that, little is known about the effect of the attachment site and linker chemistry on the bacteria staining efficiency displayed by AMP-fluorophore conjugates. Here we designed and synthesized three derivatives of the antimicrobial peptide ubiquicidin with Nile Red that differed by the position and chemistry of bioconjugation. We showed that the internally labeled probe that incorporated the fluorophore in the form of a minimalistic non-canonical α-amino acid was superior to the probes obtained by more traditional N-terminus labeling and lysine side-chain labeling approaches. The internally labeled probe enabled rapid wash-free fluorescence staining of Gram-positive and Gram-negative bacteria and their detection in an add-and-read format by fluorescence microscopy and flow cytometry.

Results

Design and synthesis of the fluorescent peptides. Numerous AMPs with distinct selectivity profiles have been used as parts of biosensors.[42–44] Among them, ubiquicidin has received much attention as a broad-spectrum bacteria-targeting molecular vector. Ubiquicidin was originally identified in murine macrophages as a cationic AMP of 59 amino acids with a sequence derived from the ribosomal protein S30.[51] Synthetic ubiquicidin and its fragments retain various degrees of antimicrobial activity.[52] Ubiquicidin and its synthetic derivatives non-covalently bind to a wide range of Gram-positive and Gram-negative bacteria, including human pathogens. The binding mechanism is presumably based on the electrostatic interactions between the positively charged side chains of the peptide and the negatively charged bacterial membranes.[53] As a result, ubiquicidin derivatives labeled with fluorescent reporters[46,50,54,55] or radioligands[56–60] have been exploited in the diagnostics and treatment of bacterial infections.[61,62] We hypothesized that ubiquicidin can be converted to a red fluorogenic probe suitable for one-step wash-free staining of bacteria. To achieve this goal, an appropriate environmentally sensitive fluorophore should be conjugated to ubiquicidin to render the peptide conditionally fluorescent while preserving its binding towards the broad range of bacteria. Nile Red (**NR**, Figure S1A) seemed a fitting fluorophore to accomplish this objective. **NR** is a neutral hydrophobic fluorophore that fluoresces in the red spectral region and exhibits an environmentally sensitive emission due to the charge transfer character of the excited state.[63] **NR** displays a significant hypsochromic shift in emission and a strong fluorescence enhancement upon transition from aqueous to hydrophobic environments. The environmental sensitivity makes **NR** a potent probe for biological systems and an attractive reporter moiety for targeted fluorogenic probes.[64] When **NR** is covalently tethered to a ligand, the resulting conjugates exhibit low fluorescence in the free form where the fluorophore is exposed to the aqueous media. At the same time, their fluorescence increases significantly upon binding to the corresponding macromolecular target, where the fluorophore becomes partially screened from the polar environment.[65–67] To incorporate the **NR** fluorophore in ubiquicidin, we employed several approaches. First, for internal labeling, we used our recently reported **NR**-based fluorescent unnatural amino acid **Alared** (Figure S1A), which has been successfully incorporated in bioactive peptides for the labeling of G protein-coupled receptors in living cells under no-wash conditions.[68] Like the parent fluorophore, **Alared** exhibits polarity-dependent changes in the fluorescence spectra, with an increasing batochromic shift and suppressed fluorescence intensity upon transition from organic solvents to water (Figure S1B). Second, we used **NR** in the form of carboxylic acid (**NR-COOH**, Figure S1A) for the N-terminal or side-chain labeling of ubiquicidin.

To study the effect of the conjugation method on the staining of bacteria, we designed three ubiquicidin analogs bearing covalently incorporated **NR** moieties. The peptide design stemmed from the existing literature data on the fluorescence labeling of ubiquicidin. We focused on the truncated version of ubiquicidin named Ubi29-41 composed of thirteen amino acids. Ubi29-41 has received much attention as a vector for infection imaging probes.[46,50,54,55] The fragment containing six positively charged residues was predicted to be disordered in solution (Figure S2). This pointed

toward the possibility that the insertion of the fluorophore into the sequence could be tolerated because it did not destabilize any pre-existing secondary structure.

The structures of the Ubi29-41-based probes are shown in Figure 1A. The internally labeled probe named **UNR-1** was obtained by incorporating **Alared** at the Y38 position, the only position that contained a natural aromatic amino acid. In addition to the Y38**Alared** mutation, **UNR-1** and the other synthesized peptides contained the norleucine (Nle) substitution of methionine at position 36, which has been shown to improve the stability of the peptide.[46] The end-labeled version of Ubi29-49 named **UNR-2** was obtained by incorporating the carboxylic derivative of **NR** at the N-terminus. The same carboxylic derivative was used to label the side-chain amino group of an internal lysine residue, resulting in the probe named **UNR-3**. The **NR**-labeled peptides were synthesized using a combination of automated and manual solid-phase peptide synthesis following the Fmoc/tBu strategy. The peptides were purified by reverse-phase semi-preparative HPLC. Their purity and identity were confirmed by HPLC and HRMS (see Supporting Information for the experimental details).

Spectroscopic characterization of the fluorescent peptides. The absorption and emission properties of fluorescent peptides were similar to those of the parent fluorophore (**NR**) under identical conditions (Figure S3 and Table S1). No blue shift was observed in the emission of **UNR-1** compared to **NR**. This observation indicated that within the internally labeled peptide, the fluorophore was fully exposed to the polar aqueous environment, which is in agreement with the predicted unstructured character of this fragment (Figure S2).

Next, we examined the fluorogenicity of the **NR**-labeled peptides. Several factors contribute to the fluorogenic properties of the **NR**-based probes.[65,66] First, the fluorogenic effect arises from the strong increase of fluorescence quantum yield in apolar and aprotic environment (Figure S3). The second factor contributing to the fluorogenicity of the **NR**-based probes is a substantial positive solvatochromism in absorption spectra, which is seen by a red shift (~ 80 nm) of the absorption maximum of the fluorophore upon transition from apolar solvents to water (Figure S4A). The amplitude of this change in relative absorption depends on the excitation wavelength (Figure S4B). For instance, the relative absorption of **NR** between water and 1,4-dioxane undergoes a 4.2-fold increase at 488 nm, 2.3-fold increase at 520 nm, and 3.5-fold decrease at 561 nm. The same combination of factors takes place for the labeled peptides (Figure 1B) and can potentially modulate the apparent brightness of the fluorescent probe upon binding to the target. To quantify the combined effect exerted by the changes in absorption and quantum yields, we measured the total fluorescence (fluorescence intensity integrated across the entire emission spectrum) of the parent fluorophore **NR** and the labeled peptides under various conditions. We used a small set of organic solvents (DMSO, EtOH, MeOH) and aqueous solutions (neat water, PBS, and a rich medium for bacterial growth). We performed measurements at three excitation wavelengths that are typically used in fluorescence readers and are compatible with **NR** (488, 520 and 561 nm). The results are presented in Figure 1C. The overall pattern in the data showed that all four compounds fluoresce better in organic solvents than in aqueous solutions. Similar trends were observed for the peptides compared with the free fluorophore, implying that the peptides maintain the fluorogenic character of **NR**. The consistent pattern observed in the data across all

experimental conditions suggests that **UNR-1**, **UNR-2** and **UNR-3** are capable of exhibiting a fluorogenic response upon binding to macromolecular targets.

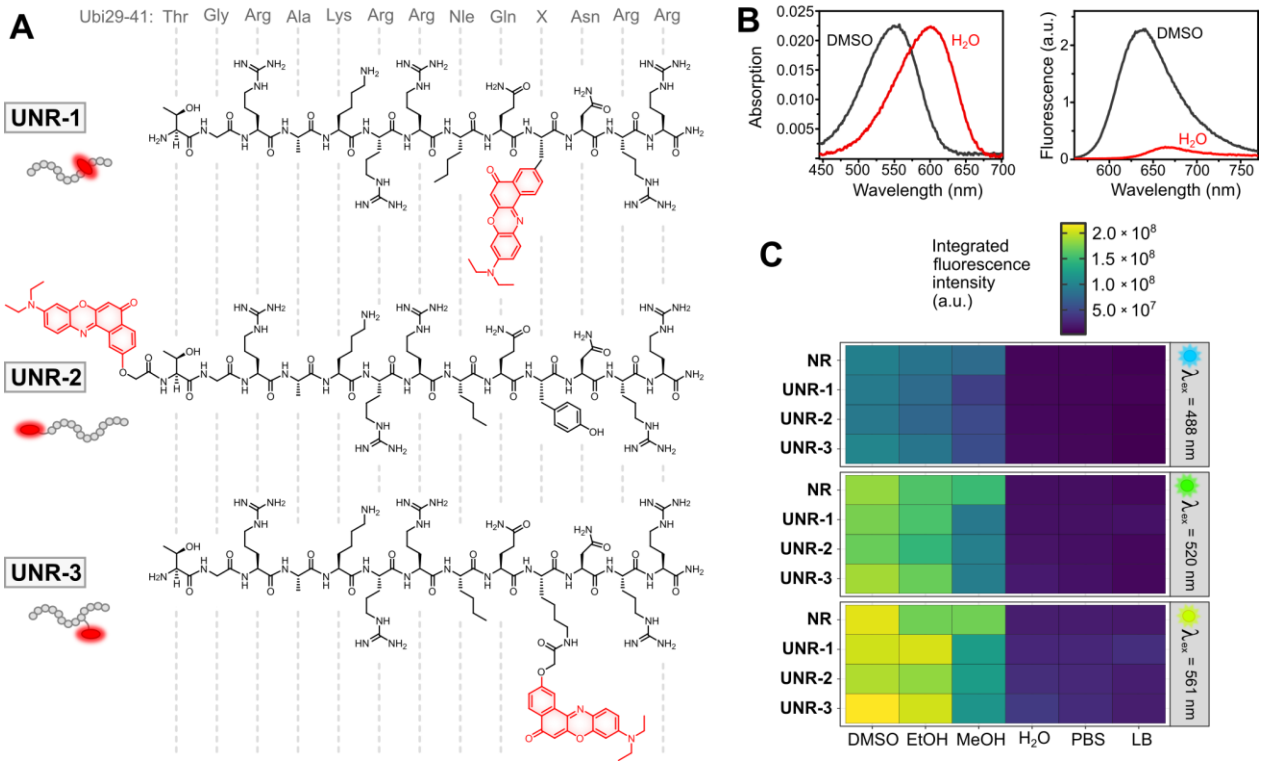

Figure 1. **A**) Structure of the Nile Red-labeled peptidic fluorescent probes **UNR-1**, **UNR-2** and **UNR-3** derived from the Ubi29-41 fragment of the antimicrobial peptide ubiquicidin; the consensus amino acid sequence of the probes is indicated on top, X designates the position of internal amino acid modifications; the Nile Red residue is shown in red. **B**) Absorption (left) and fluorescence emission (right) spectra of a 1 μM solution of **UNR-1** in DMSO and water; λ_{ex} = 520 nm. **C**) Background-corrected integrated fluorescence intensities of 1 μM solutions of **NR** and the probes **UNR-1**, **UNR-2** and **UNR-3** in different organic solvents and aqueous solutions upon excitation at 488 nm, 520 nm, and 561 nm. PBS = phosphate-buffered saline; LB = Luria-Bertani medium.

Analysis of stained bacteria by flow cytometry. We examined the possibility of direct add-and-read staining of live bacteria with the new peptidic probes. We used *B. subtilis* and *E. coli* as representative Gram-positive and Gram-negative bacteria, respectively. We shortly incubated live *B. subtilis* and *E. coli* cells in the early logarithmic growth phase with the peptidic probes in LB growth medium and then directly injected bacteria into a flow cytometer without washing out the unbound probe. The incubation of the bacteria with **UNR-1**, **UNR-2** and **UNR-3** resulted in a significant increase in the mean fluorescence intensity upon excitation at 488 nm and fluorescence detection using a red emission filter (Figure 2A). Having confirmed the compatibility of our probes with flow cytometry measurements, we then examined whether the observed fluorescence

intensity of the stained bacterial population depended on the concentration of the probe in solution. To solidify our conclusions, we included *Staphylococcus epidermidis* and *Pseudomonas stutzeri* as additional Gram-positive and Gram-negative bacterial strains, respectively. **NR** was used as a non-specific control. The results are shown in Figure 2B. The internally labeled probe **UNR-1** stained all the tested strains in a concentration-dependent manner (Figure 2B). The same tendency was observed for **UNR-2** and **UNR-3**, albeit with significantly diminished fluorescence intensities. The non-targeted dye **NR** stained the Gram-positive bacteria with a similar efficiency than **UNR-1**, whereas much weaker efficiency was observed for the Gram-negative strains *E. coli* and *P. stutzeri*. The flow cytometry data indicated that, among the tested fluorescent labels, **UNR-1** was the most efficient one, as it stained both Gram-positive and Gram-negative bacterial cells in solution at reasonable probe concentrations (1–10 µM) and short incubation times of a few minutes. The concentrations used for staining are significantly lower than the minimal inhibitory concentration (MIC) determined for the non-modified parent peptide Ubi29-41 M36Nle (>64 $\mu g \cdot mL^{-1}$). For further experiments, we focused on **UNR-1** as the most efficient probe.

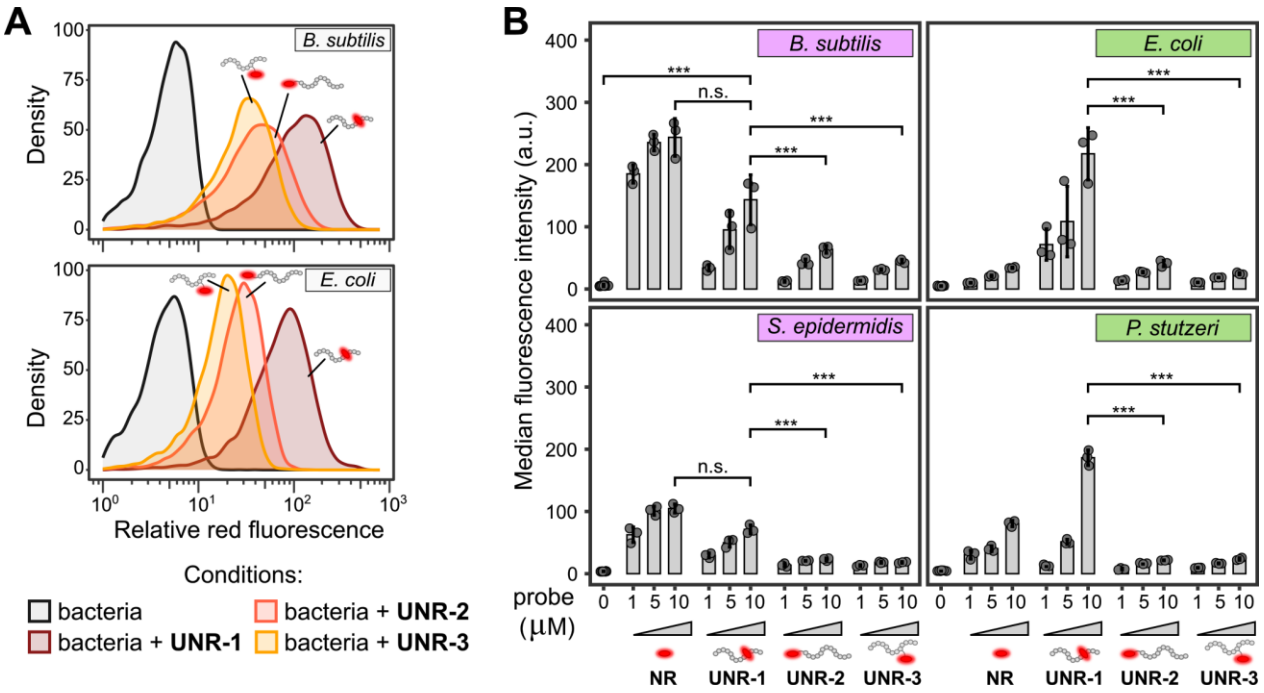

Figure 2. Flow cytometry analysis of bacteria stained with **NR** and the **NR**-labeled peptidic probes. **A**) Flow cytometry profiles of the representative Gram-positive and Gram-negative bacteria incubated with the peptidic probes **UNR-1**, **UNR-2** and **UNR-3**; the labeling was performed under no-wash conditions by adding the probe (5 µM) to the bacteria in the early logarithmic phase shortly before measurements; excitation wavelength was 488 nm; fluorescence was detected using a 680/30 emission filter. **B**) Mean of median fluorescence intensities of the bacteria stained with 1, 5, and 10 µM of **NR** and the **NR**-based peptides under no-wash conditions; error bars represent standard deviation for n ≥ 3 biological replicates; the Kruskal–Wallis test followed by multiple Wilcoxon–Mann–Whitney tests with p-value adjustment; *** $p < 0.001$, n.s = non-significant.

Next, we used flow cytometry to examine the ability of **UNR-1** to stain bacteria that were inactivated by heat or by paraformaldehyde (PFA). The probe sufficiently stained both *B. subtilis* and *E. coli* that were inactivated by heating at 90 ºC for 15 min, with overall higher median fluorescence intensity than for live bacteria (Figure S5). In addition, **UNR-1** stained paraformaldehyde-fixed bacteria, although the results depended on the fixation protocol (Figure S6). Low fluorescence was observed when cells were fixed with PFA after labeling with **UNR-1**, likely due to the dissociation of the probe during washings (Figure S6A). Fixation followed by labeling in phosphate-buffered saline resulted in robustly high staining for both the Gram-positive and Gram-negative bacteria (Figure S6B). The observed increase in fluorescence cannot be attributed to the change of the buffer alone because the incubation of the probe with live bacteria in PBS gave a significantly lower fluorescence intensity (Figure S6C).

Finally, in a proof-of-concept experiment, we examined the ability of **UNR-1** to stain bacteria directly in biological liquids using urine as example. Bacteriuria is the presence of bacteria in urine at a level of $\geq 10^5$ bacteria·mL^{-1}.[69] Fast detection of bacteria in urine is important for the diagnosis of urinary tract infections (UTIs) and other disorders. We added **UNR-1** (5 µM) to *E. coli*-inoculated urine samples and directly analyzed them by flow cytometry. In one case, sterile urine was freshly inoculated with *E. coli* previously grown in LB. In the second case, *E. coli* was grown in sterile urine overnight. In both cases, bacteria were robustly stained (Figure S7), validating the potential of **UNR-1** as a probe for the detection of bacteria in biological liquids. Altogether, the results of flow cytometry experiments showed that **UNR-1** is a convenient fluorescent probe for staining both live and dead Gram-negative and Gram-positive bacteria and for detecting them in an add-and-read format.

Selectivity of the probe. We used fluorescence microscopy to characterize the selectivity of **UNR-1** for the bacteria versus the mammalian cells. We incubated live *E. coli* K-12 cells with 1 µM of **UNR-1** in the growth medium and then imaged them under no-wash conditions. Cells were co-stained with a blue fluorescent DNA-specific dye. Cultured adherent mammalian cells (HEK 293T) were used for comparison. The parent dye (**NR**), known to non-selectively stain lipid membranes and other hydrophobic cellular structures in eukaryotic cells, was used as a control. Imaging was performed on a confocal fluorescence microscope using identical excitation and emission settings for each channel. The results are shown in Figure 3. As expected, unconjugated **NR** non-selectively stained the cytoplasmic and internal lipid membranes in HEK 293T cells, including the nuclear membrane. At the same time, the incubation of live *E. coli* with **NR** resulted in a dim diffuse signal that was not associated with the cells, likely due to the poor permeability of the outer membrane of Gram-negative bacteria for exogenous molecules. The inverse staining pattern was observed with **UNR-1**. We observed that the **NR**-labeled peptide stained the bacteria but not the eukaryotic cells. A sufficient level of contrast was observed in the presence of the unbound peptide in solution (no-wash conditions). These observations confirmed the possibility of detecting bacteria under no-wash conditions due to the bacteria-targeting properties of the peptide vector and the fluorogenic nature of the probe.

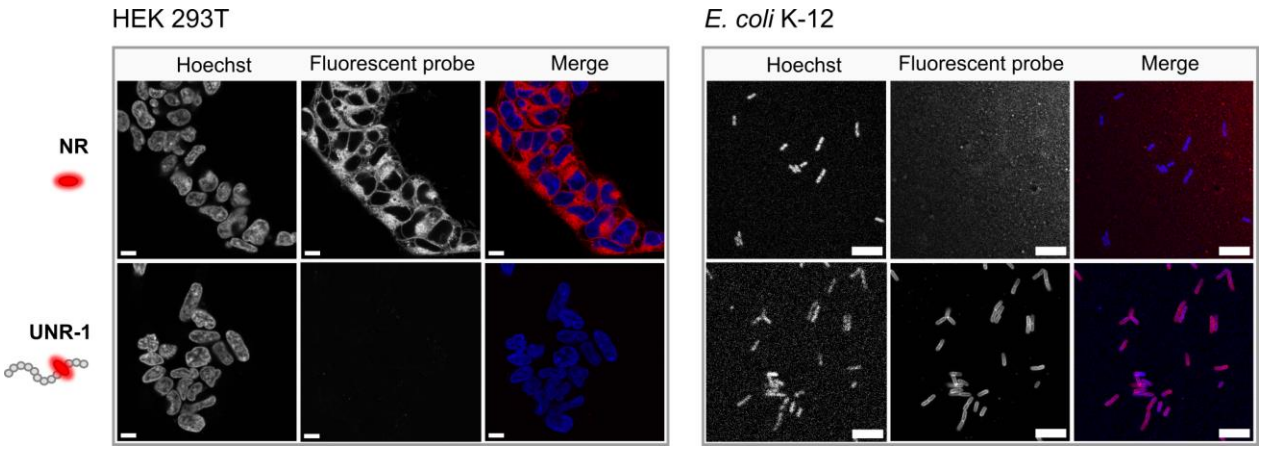

Figure 3. Confocal fluorescence microscopy images of live HEK 293T and *E. coli* K-12 cells stained with 1 μM of **NR** or **UNR-1** under no-wash conditions (λ_{ex} = 561 nm, λ_{em} = 570–730 nm). The cellular DNA was stained with Hoechst 33342 (λ_{ex} = 405 nm, λ_{em} = 430–480 nm). The images in each channel were recorded using identical instrumental settings. Representative images of at least two independent replicates. Scale bars, 10 μm.

***Study of the localization of UNR-1 in bacteria*.** To reveal the localization of **UNR-1** in bacteria, we first tested the compatibility of our probes with super-resolution microscopy. Incubation of live bacteria with **UNR-1** resulted in spontaneous fluorescence blinking observed on the millisecond time scale (data not shown). The most probable explanation of the "on" events was the transient immobilization of the peptide upon binding to the cell in combination with the increased brightness of the bound probe. The "off" events likely occurred due to dissociation of the probe or photobleaching. Analogously to **NR** and its derivatives,[70,71] the blinking behavior of **UNR-1** made the probe compatible with single-molecule localization microscopy (SMLM). The on/off switching of **UNR-1** enabled recording of individual molecular localizations over a period of time followed by reconstructing a sub-diffraction image of the labeled cell. Using an SMLM setup[72] (Figure 4A), we imaged *E. coli* and *B. subtilis* as representative Gram-positive and Gram-negative bacteria (Figures 4B and 4C, respectively). The average localization accuracy was around 21–24 nm (Figure S8). The observed characteristic structures indicated that the probe was bound to the surface of cells.

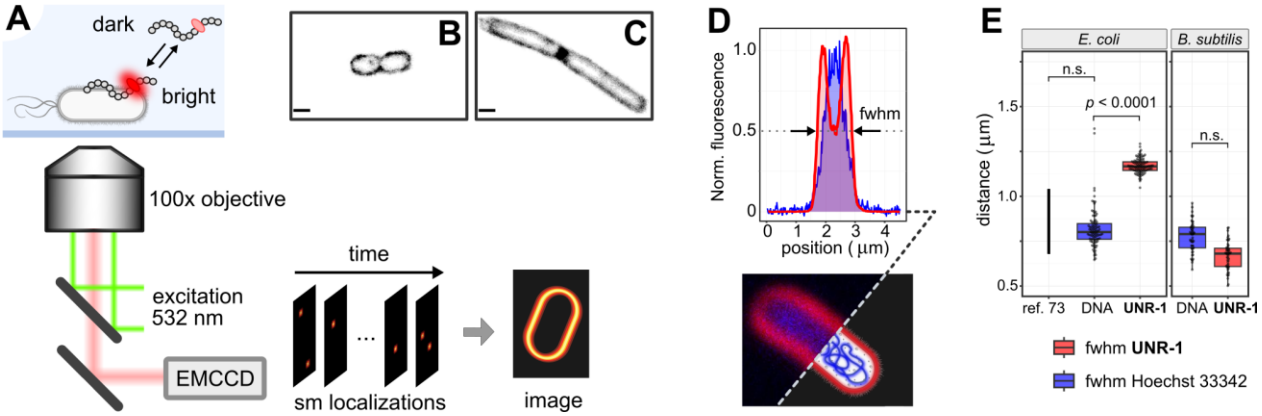

Figure 4. **A)** Single-molecule localization microscopy with **UNR-1**. **B–C)** Super-resolution fluorescence microscopy images of **UNR-1**-labeled *E. coli* (**B**) and *B. subtilis* (**C**); scale bars, 1 µm. **D**) Normalized fluorescence intensity profiles obtained from two-color confocal fluorescence images of bacteria co-labeled with **UNR-1** (red) and Hoechst 33342 (blue); fwhm = full width at half-maximum. **E**) Comparison of the fwhm values of the red and blue fluorescence intensity profiles for *E. coli* and *B. subtilis* (*n* >50 cells, one-tailed Wilcoxon–Mann–Whitney test, n.s. = non-significant); reference diameter of *E. coli* cells was taken from ref.[73]

We performed an additional experiment to more specifically characterize the localization of the probe in *E. coli* and *B. subtilis*. We hypothesized that insights into the localization of the probe with respect to the bacterial plasma membrane could be obtained from the analysis of cells co-labeled with **UNR-1** and a DNA-specific fluorescent dye. Because the cellular DNA is contained within the uncompartmentalized cytoplasm, the DNA-associated fluorescence signal should mark the internal volume of the cell. Comparing the dimensions of the DNA and **UNR-1** fluorescence blobs in diffraction-limited images, one can conclude whether the probe is localized in proximity to the cytoplasm, at the plasma membrane, or the periphery of the cell bound to the outer layers of the cell wall. To analyze the probe location, we perpendicularly sectioned the bicolor confocal fluorescence images of bacteria and measured the full width at half-maximum (fwhm) of the normalized fluorescence signal for each fluorophore (Figure 4D). For *E. coli*, the measured mean value of fwhm for the DNA stain was ~ 0.79 µm. This distribution of fwhm values matched well the reference diameter range of the bacterium that was measured by electron microscopy under different growth conditions (Figure 4E).[73] Meanwhile, the fwhm of the red signal generated by **UNR-1** was significantly larger, with a mean value of ~ 1.17 µm (Figure 4E). On the contrary, for *B. subtilis,* the fwhm of the **UNR-1** signal did not exceed significantly the fwhm of the intracellular signal associated with DNA. This indicated that in the case of *E. coli,* the peptide probe was most likely bound to the outer layers of the cell wall, such as the outer membrane. In the case of *B. subtilis* the probe resided in close proximity to the cytoplasm, most likely bound to the plasma membrane. This result is consistent with the known mechanism of action of Ubi29-41, which does not cross the cell wall barriers and interacts with the external negatively charged membrane surfaces.[53]

Discussion

The fluorogenicity of **NR** and its compatibility with the conditions of Fmoc/tBu solid-phase peptide synthesis and purification make this fluorophore a promising building block for the design of peptide-based fluorescent probes emitting in the red region of the spectrum. Several such probes based on **NR** have been reported.[65,67] Typically, the fluorophore was introduced at the N-terminus or a lysine side chain of a synthetic peptide via an amide bond. There has been scarce knowledge about the effect of the fluorophore attachment site and chemistry on the performance of the labeled probes. To address this problem, we synthesized and compared three bacteria-targeting peptidic probes based on the **NR** fluorophore using different bioconjugation methods. The synthesized probes contained fluorophore either in the form of an internal unnatural amino acid (**UNR-1**), in the form of an N-terminal label (**UNR-2**), or the form of a lysine side-chain modification (**UNR-3**). We observed no effect of the fluorophore attachment on the intrinsic fluorogenicity of the probes, where all the labeled peptides showed similar fluorescence change patterns. However, the probes differed dramatically in their bacteria staining efficiency. The backbone-labeled probe **UNR-1** incorporating the fluorophore in the form of unnatural amino acid **Alared** yielded a significantly higher fluorescence signal than the probes labeled with more traditional approaches. Our results suggest that the backbone labeling approach based on fluorescent unnatural amino acids deserves more attention upon the development of fluorescent probes based on **NR** and other environmentally sensitive fluorophores.

The ability of the new probes to fluorescently stain bacteria and their selectivity over mammalian cells have corroborated the potency of ubiquicidin as a bacteria-targeting molecular vector. The capacity of the probe to stain bacteria *in situ* without washing in aqueous media opens many avenues for future practical applications. For instance, **UNR-1** could be used for rapid detection of bacteria in biological and environmental samples. If combined with an appropriate enrichment method and fluorescence readout device, the probe could be used for the detection of low levels of bacterial pathogens in medical laboratory diagnostics. Unlike the fluorescence staining methods based on metabolic labeling of bacterial polymers, **UNR-1** does not rely on bacterial enzymes. Therefore, this new probe could find applications in staining and detection of viable but nonculturable (VBNC) bacteria, metabolically dormant persister cells, bacterial spores, etc. Finally, the probe could be used for fluorescence staining of bacteria-derived nanostructures, such as various types of bacterial outer membrane vesicles (OMVs). Further research in these directions is ongoing in our laboratories.

Conclusion

We designed three fluorogenic bacteria-targeting peptides by conjugating Nile Red at different sites of the antimicrobial peptide Ubi29-41. While displaying similar fluorescence properties in solutions, the labeled peptides differed significantly in their ability to stain bacteria. The peptide probe **UNR-1** incorporating the fluorophore in the form of a minimalistic unnatural amino acid **Alared** stained both Gram-positive and Gram-negative bacteria with greater efficiency. The staining was performed in an add-and-read format in a variety of liquid samples. The probe was

used to quickly stain and detect bacteria with fluorescence microscopy and flow cytometry, implying potential applications in basic research and diagnostics.

Associated content

Supporting Information

Figures S1–S8, table S1, synthesis and characterization of the peptides, experimental details for spectroscopy, microscopy, flow cytometry, and data analysis.

Acknowledgement

This work of the Strasbourg Drug Discovery and Development Institute (IMS), as part of the Interdisciplinary Thematic Institute (ITI) 2021−2028 program of the University of Strasbourg, CNRS, and Inserm, was supported by IdEx Unistra (ANR-10-IDEX-0002) and by the SFRI-STRAT'US project (ANR-20-SFRI-0012) under the framework of the French Investments for the Future Program. This work was also supported by IdEx Unistra 2022 "Recherche exploratoire", IdEx Unistra 2019 "Post-doctorants", ANR-22-CE44-0033 ULTRON, the CNRS through the MITI interdisciplinary programs "Lumière et vie", and the University of Strasbourg. L.W. and L.B. were supported by fellowships from the French Ministry of Higher Education, Research and Innovation. We are grateful to Prof. Valérie Geoffroy (CNRS UMR7242 BSC) for the gift of *P. stutzeri*, Christel Valencia (PCBIS, UAR 3286) for providing HEK 293T cells, Dr. Delphine Garnier, Dr Estefanía Olivia and Dr. Cheng Deng (PACSI platform GDS3670) for mass spectrometry, Romain Vauchelles (PIQ-QuESt platform, member of the national infrastructure France-BioImaging supported by the French National Research Agency (ANR-10-INBS-04)) for the assistance in the microscopy experiments, Dr. Nicolas Humbert (UMR 7021 and Plateforme de Spectroscopie et de Synthèse Peptidique) for the assistance in the fluorescence spectroscopy experiments.

Author information

* Corresponding authors

E-mail: julie.karpenko@unistra.fr dmytro.dziuba@unistra.fr

Notes

# These authors contributed equally to the work. The authors declare no competing financial interest.

References

(1) Akram, F.; Imtiaz, M.; Haq, I. U. Emergent Crisis of Antibiotic Resistance: A Silent Pandemic Threat to 21st Century. *Microbial Pathogenesis* **2023**, *174*, 105923. https://doi.org/10.1016/j.micpath.2022.105923.

(2) Thornber, K.; Kirchhelle, C. Hardwiring Antimicrobial Resistance Mitigation into Global Policy. *JAC-Antimicrobial Resistance* **2022**, *4* (4), dlac083. https://doi.org/10.1093/jacamr/dlac083.

(3) Baker, S. J.; Payne, D. J.; Rappuoli, R.; De Gregorio, E. Technologies to Address Antimicrobial Resistance. *Proc Natl Acad Sci U S A* **2018**, *115* (51), 12887–12895. https://doi.org/10.1073/pnas.1717160115.

(4) Ahmed, A.; Rushworth, J. V.; Hirst, N. A.; Millner, P. A. Biosensors for Whole-Cell Bacterial Detection. *Clin Microbiol Rev* **2014**, *27* (3), 631–646. https://doi.org/10.1128/CMR.00120-13.

(5) Reynoso, E. C.; Laschi, S.; Palchetti, I.; Torres, E. Advances in Antimicrobial Resistance Monitoring Using Sensors and Biosensors: A Review. *Chemosensors* **2021**, *9* (8), 232. https://doi.org/10.3390/chemosensors9080232.

(6) Vidic, J.; Manzano, M. Electrochemical Biosensors for Rapid Pathogen Detection. *Current Opinion in Electrochemistry* **2021**, *29*, 100750. https://doi.org/10.1016/j.coelec.2021.100750.

(7) Wang, P.; Sun, H.; Yang, W.; Fang, Y. Optical Methods for Label-Free Detection of Bacteria. *Biosensors* **2022**, *12* (12), 1171. https://doi.org/10.3390/bios12121171.

(8) Tallury, P.; Malhotra, A.; Byrne, L. M.; Santra, S. Nanobioimaging and Sensing of Infectious Diseases. *Advanced Drug Delivery Reviews* **2010**, *62* (4–5), 424–437. https://doi.org/10.1016/j.addr.2009.11.014.

(9) Vidic, J.; Manzano, M.; Chang, C.-M.; Jaffrezic-Renault, N. Advanced Biosensors for Detection of Pathogens Related to Livestock and Poultry. *Vet Res* **2017**, *48* (1), 11. https://doi.org/10.1186/s13567-017-0418-5.

(10) Pulido, M. R.; Garcia-Quintanilla, M.; Martin-Pena, R.; Cisneros, J. M.; McConnell, M. J. Progress on the Development of Rapid Methods for Antimicrobial Susceptibility Testing. *Journal of Antimicrobial Chemotherapy* **2013**, *68* (12), 2710–2717. https://doi.org/10.1093/jac/dkt253.

(11) Sin, M. L.; Mach, K. E.; Wong, P. K.; Liao, J. C. Advances and Challenges in Biosensor-Based Diagnosis of Infectious Diseases. *Expert Review of Molecular Diagnostics* **2014**, *14* (2), 225–244. https://doi.org/10.1586/14737159.2014.888313.

(12) Li, B.; Yu, Q.; Duan, Y. Fluorescent Labels in Biosensors for Pathogen Detection. *Critical Reviews in Biotechnology* **2015**, *35* (1), 82–93. https://doi.org/10.3109/07388551.2013.804487.

(13) Huang, Y.; Chen, W.; Chung, J.; Yin, J.; Yoon, J. Recent Progress in Fluorescent Probes for Bacteria. *Chem. Soc. Rev.* **2021**, *50* (13), 7725–7744. https://doi.org/10.1039/D0CS01340D.

(14) Zhang, J.; Zhou, M.; Li, X.; Fan, Y.; Li, J.; Lu, K.; Wen, H.; Ren, J. Recent Advances of Fluorescent Sensors for Bacteria Detection-A Review. *Talanta* **2023**, *254*, 124133. https://doi.org/10.1016/j.talanta.2022.124133.

(15) Kong, Y.; Jiang, Q.; Zhang, F.; Yang, Y. Small Molecular Fluorescent Probes: Application Progress of Specific Bacteria Detection and Antibacterial Phototherapy. *Chemistry An Asian Journal* **2023**, *18* (11), e202300178. https://doi.org/10.1002/asia.202300178.

(16) Wang, Z.; Xing, B. Small-Molecule Fluorescent Probes: Big Future for Specific Bacterial Labeling and Infection Detection. *Chem. Commun.* **2022**, *58* (2), 155–170. https://doi.org/10.1039/D1CC05531C.
(17) Mills, B.; Bradley, M.; Dhaliwal, K. Optical Imaging of Bacterial Infections. *Clin Transl Imaging* **2016**, *4* (3), 163–174. https://doi.org/10.1007/s40336-016-0180-0.
(18) Li, X.; Gao, X.; Shi, W.; Ma, H. Design Strategies for Water-Soluble Small Molecular Chromogenic and Fluorogenic Probes. *Chem. Rev.* **2014**, *114* (1), 590–659. https://doi.org/10.1021/cr300508p.
(19) Chyan, W.; Raines, R. T. Enzyme-Activated Fluorogenic Probes for Live-Cell and *in Vivo* Imaging. *ACS Chem. Biol.* **2018**, *13* (7), 1810–1823. https://doi.org/10.1021/acschembio.8b00371.
(20) Li, C.; Tebo, A.; Gautier, A. Fluorogenic Labeling Strategies for Biological Imaging. *IJMS* **2017**, *18* (7), 1473. https://doi.org/10.3390/ijms18071473.
(21) Kobayashi, H.; Ogawa, M.; Alford, R.; Choyke, P. L.; Urano, Y. New Strategies for Fluorescent Probe Design in Medical Diagnostic Imaging. *Chem. Rev.* **2010**, *110* (5), 2620–2640. https://doi.org/10.1021/cr900263j.
(22) Zhang, Y.; Zhang, G.; Zeng, Z.; Pu, K. Activatable Molecular Probes for Fluorescence-Guided Surgery, Endoscopy and Tissue Biopsy. *Chem. Soc. Rev.* **2022**, *51* (2), 566–593. https://doi.org/10.1039/D1CS00525A.
(23) Wu, X.; Wang, R.; Kwon, N.; Ma, H.; Yoon, J. Activatable Fluorescent Probes for *in Situ* Imaging of Enzymes. *Chem. Soc. Rev.* **2022**, *51* (2), 450–463. https://doi.org/10.1039/D1CS00543J.
(24) Manafi, M.; Kneifel, W.; Bascomb, S. Fluorogenic and Chromogenic Substrates Used in Bacterial Diagnostics. *Microbiol Rev* **1991**, *55* (3), 335–348. https://doi.org/10.1128/mr.55.3.335-348.1991.
(25) Rajapaksha, P.; Elbourne, A.; Gangadoo, S.; Brown, R.; Cozzolino, D.; Chapman, J. A Review of Methods for the Detection of Pathogenic Microorganisms. *Analyst* **2019**, *144* (2), 396–411. https://doi.org/10.1039/C8AN01488D.
(26) Liu, W.; Miao, L.; Li, X.; Xu, Z. Development of Fluorescent Probes Targeting the Cell Wall of Pathogenic Bacteria. *Coordination Chemistry Reviews* **2021**, *429*, 213646. https://doi.org/10.1016/j.ccr.2020.213646.
(27) Kocaoglu, O.; Carlson, E. E. Progress and Prospects for Small-Molecule Probes of Bacterial Imaging. *Nat Chem Biol* **2016**, *12* (7), 472–478. https://doi.org/10.1038/nchembio.2109.
(28) Parker, M. F. L.; Flavell, R. R.; Luu, J. M.; Rosenberg, O. S.; Ohliger, M. A.; Wilson, D. M. Small Molecule Sensors Targeting the Bacterial Cell Wall. *ACS Infect. Dis.* **2020**, *6* (7), 1587–1598. https://doi.org/10.1021/acsinfecdis.9b00515.
(29) Geva-Zatorsky, N.; Alvarez, D.; Hudak, J. E.; Reading, N. C.; Erturk-Hasdemir, D.; Dasgupta, S.; Von Andrian, U. H.; Kasper, D. L. In Vivo Imaging and Tracking of Host–Microbiota Interactions via Metabolic Labeling of Gut Anaerobic Bacteria. *Nat Med* **2015**, *21* (9), 1091–1100. https://doi.org/10.1038/nm.3929.
(30) Dumont, A.; Malleron, A.; Awwad, M.; Dukan, S.; Vauzeilles, B. Click-Mediated Labeling of Bacterial Membranes through Metabolic Modification of the Lipopolysaccharide Inner Core. *Angew Chem Int Ed* **2012**, *51* (13), 3143–3146. https://doi.org/10.1002/anie.201108127.

(31) Radkov, A. D.; Hsu, Y.-P.; Booher, G.; VanNieuwenhze, M. S. Imaging Bacterial Cell Wall Biosynthesis. *Annu. Rev. Biochem.* **2018**, *87* (1), 991–1014. https://doi.org/10.1146/annurev-biochem-062917-012921.

(32) Marshall, A. P.; Shirley, J. D.; Carlson, E. E. Enzyme-Targeted Fluorescent Small-Molecule Probes for Bacterial Imaging. *Current Opinion in Chemical Biology* **2020**, *57*, 155–165. https://doi.org/10.1016/j.cbpa.2020.05.012.

(33) Kwon, H.; Liu, X.; Choi, E. G.; Lee, J. Y.; Choi, S.; Kim, J.; Wang, L.; Park, S.; Kim, B.; Lee, Y.; Kim, J.; Kang, N. Y.; Chang, Y. Development of a Universal Fluorescent Probe for Gram-Positive Bacteria. *Angew Chem Int Ed* **2019**, *58* (25), 8426–8431. https://doi.org/10.1002/anie.201902537.

(34) Mason, D. J.; Shanmuganathan, S.; Mortimer, F. C.; Gant, V. A. A Fluorescent Gram Stain for Flow Cytometry and Epifluorescence Microscopy. *Appl Environ Microbiol* **1998**, *64* (7), 2681–2685. https://doi.org/10.1128/AEM.64.7.2681-2685.1998.

(35) Leevy, W. M.; Johnson, J. R.; Lakshmi, C.; Morris, J.; Marquez, M.; Smith, B. D. Selective Recognition of Bacterial Membranes by Zinc(Ii)-Coordination Complexes. *Chem. Commun.* **2006**, No. 15, 1595. https://doi.org/10.1039/b517519d.

(36) Guilini, C.; Baehr, C.; Schaeffer, E.; Gizzi, P.; Rufi, F.; Haiech, J.; Weiss, E.; Bonnet, D.; Galzi, J.-L. New Fluorescein Precursors for Live Bacteria Detection. *Anal. Chem.* **2015**, *87* (17), 8858–8866. https://doi.org/10.1021/acs.analchem.5b02100.

(37) Stone, M. R. L.; Butler, M. S.; Phetsang, W.; Cooper, M. A.; Blaskovich, M. A. T. Fluorescent Antibiotics: New Research Tools to Fight Antibiotic Resistance. *Trends Biotechnol* **2018**, *36* (5), 523–536. https://doi.org/10.1016/j.tibtech.2018.01.004.

(38) Geng, T.; Uknalis, J.; Tu, S.-I.; Bhunia, A. Fiber-Optic Biosensor Employing Alexa-Fluor Conjugated Antibody for Detection of Escherichia Coli O157:H7 from Ground Beef in Four Hours. *Sensors* **2006**, *6* (8), 796–807. https://doi.org/10.3390/s6080796.

(39) Wang, X.; Du, Y.; Li, Y.; Li, D.; Sun, R. Fluorescent Identification and Detection of Staphylococcus Aureus with Carboxymethyl Chitosan/CdS Quantum Dots Bioconjugates. *Journal of Biomaterials Science, Polymer Edition* **2011**, *22* (14), 1881–1893. https://doi.org/10.1163/092050610X528570.

(40) Chang, D.; Zakaria, S.; Esmaeili Samani, S.; Chang, Y.; Filipe, C. D. M.; Soleymani, L.; Brennan, J. D.; Liu, M.; Li, Y. Functional Nucleic Acids for Pathogenic Bacteria Detection. *Acc. Chem. Res.* **2021**, *54* (18), 3540–3549. https://doi.org/10.1021/acs.accounts.1c00355.

(41) Silva, R. R.; Avelino, K. Y. P. S.; Ribeiro, K. L.; Franco, O. L.; Oliveira, M. D. L.; Andrade, C. A. S. Optical and Dielectric Sensors Based on Antimicrobial Peptides for Microorganism Diagnosis. *Front. Microbiol.* **2014**, *5*. https://doi.org/10.3389/fmicb.2014.00443.

(42) Islam, M. A.; Karim, A.; Ethiraj, B.; Raihan, T.; Kadier, A. Antimicrobial Peptides: Promising Alternatives over Conventional Capture Ligands for Biosensor-Based Detection of Pathogenic Bacteria. *Biotechnology Advances* **2022**, *55*, 107901. https://doi.org/10.1016/j.biotechadv.2021.107901.

(43) Qiao, Z.; Fu, Y.; Lei, C.; Li, Y. Advances in Antimicrobial Peptides-Based Biosensing Methods for Detection of Foodborne Pathogens: A Review. *Food Control* **2020**, *112*, 107116. https://doi.org/10.1016/j.foodcont.2020.107116.

(44) Pardoux, É.; Boturyn, D.; Roupioz, Y. Antimicrobial Peptides as Probes in Biosensors Detecting Whole Bacteria: A Review. *Molecules* **2020**, *25* (8), 1998. https://doi.org/10.3390/molecules25081998.

(45) Ramos-Martín, F.; Annaval, T.; Buchoux, S.; Sarazin, C.; D'Amelio, N. ADAPTABLE: A Comprehensive Web Platform of Antimicrobial Peptides Tailored to the User's Research. *Life Sci. Alliance* **2019**, *2* (6), e201900512. https://doi.org/10.26508/lsa.201900512.

(46) Akram, A. R.; Avlonitis, N.; Lilienkampf, A.; Perez-Lopez, A. M.; McDonald, N.; Chankeshwara, S. V.; Scholefield, E.; Haslett, C.; Bradley, M.; Dhaliwal, K. A Labelled-Ubiquicidin Antimicrobial Peptide for Immediate in Situ Optical Detection of Live Bacteria in Human Alveolar Lung Tissue. *Chem. Sci.* **2015**, *6* (12), 6971–6979. https://doi.org/10.1039/C5SC00960J.

(47) Baibek, A.; Üçüncü, M.; Blackburn, E. A.; Bradley, M.; Lilienkampf, A. Wash-free, Peptide-based Fluorogenic Probes for Microbial Imaging. *Peptide Science* **2021**, *113* (1). https://doi.org/10.1002/pep2.24167.

(48) Dosselli, R.; Tampieri, C.; Ruiz-González, R.; De Munari, S.; Ragàs, X.; Sánchez-García, D.; Agut, M.; Nonell, S.; Reddi, E.; Gobbo, M. Synthesis, Characterization, and Photoinduced Antibacterial Activity of Porphyrin-Type Photosensitizers Conjugated to the Antimicrobial Peptide Apidaecin 1b. *J. Med. Chem.* **2013**, *56* (3), 1052–1063. https://doi.org/10.1021/jm301509n.

(49) Welling, M. M.; de Korne, C. M.; Spa, S. J.; van Willigen, D. M.; Hensbergen, A. W.; Bunschoten, A.; Duszenko, N.; Smits, W. K.; Roestenberg, M.; van Leeuwen, F. W. B. Multimodal Tracking of Controlled *Staphylococcus Aureus* Infections in Mice. *ACS Infect. Dis.* **2019**, *5* (7), 1160–1168. https://doi.org/10.1021/acsinfecdis.9b00015.

(50) Chen, H.; Liu, C.; Chen, D.; Madrid, K.; Peng, S.; Dong, X.; Zhang, M.; Gu, Y. Bacteria-Targeting Conjugates Based on Antimicrobial Peptide for Bacteria Diagnosis and Therapy. *Mol. Pharmaceutics* **2015**, *12* (7), 2505–2516. https://doi.org/10.1021/acs.molpharmaceut.5b00053.

(51) Hiemstra, P. S.; Van Den Barselaar, M. T.; Roest, M.; Nibbering, P. H.; Van Furth, R. Ubiquicidin, a Novel Murine Microbicidal Protein Present in the Cytosolic Fraction of Macrophages. *Journal of Leukocyte Biology* **1999**, *66* (3), 423–428. https://doi.org/10.1002/jlb.66.3.423.

(52) Brouwer, C. P. J. M.; Bogaards, S. J. P.; Wulferink, M.; Velders, M. P.; Welling, M. M. Synthetic Peptides Derived from Human Antimicrobial Peptide Ubiquicidin Accumulate at Sites of Infections and Eradicate (Multi-Drug Resistant) Staphylococcus Aureus in Mice. *Peptides* **2006**, *27* (11), 2585–2591. https://doi.org/10.1016/j.peptides.2006.05.022.

(53) Bhatt Mitra, J.; Sharma, V. K.; Mukherjee, A.; Garcia Sakai, V.; Dash, A.; Kumar, M. Ubiquicidin-Derived Peptides Selectively Interact with the Anionic Phospholipid Membrane. *Langmuir* **2020**, *36* (1), 397–408. https://doi.org/10.1021/acs.langmuir.9b03243.

(54) Akram, A. R.; Avlonitis, N.; Scholefield, E.; Vendrell, M.; McDonald, N.; Aslam, T.; Craven, T. H.; Gray, C.; Collie, D. S.; Fisher, A. J.; Corris, P. A.; Walsh, T.; Haslett, C.; Bradley, M.; Dhaliwal, K. Enhanced Avidity from a Multivalent Fluorescent Antimicrobial Peptide Enables Pathogen Detection in a Human Lung Model. *Sci Rep* **2019**, *9* (1), 8422. https://doi.org/10.1038/s41598-019-44804-0.

(55) Liu, C.; Gu, Y. NONINVASIVE OPTICAL IMAGING OF *STAPHYLOCOCCUS AUREUS* INFECTION *IN VIVO* USING AN ANTIMICROBIAL PEPTIDE FRAGMENT BASED NEAR-INFRARED FLUORESCENT PROBES. *J. Innov. Opt. Health Sci.* **2013**, *06* (03), 1350026. https://doi.org/10.1142/S1793545813500260.

(56) Akhtar, M. S.; Imran, M. B.; Nadeem, M. A.; Shahid, A. Antimicrobial Peptides as Infection Imaging Agents: Better Than Radiolabeled Antibiotics. *International Journal of Peptides* **2012**, *2012*, 1–19. https://doi.org/10.1155/2012/965238.

(57) Akhtar, M. S.; Qaisar, A.; Irfanullah, J.; Iqbal, J.; Khan, B.; Jehangir, M.; Nadeem, M. A.; Khan, M. A.; Afzal, M. S.; Ul-Haq, I.; Imran, M. B. Antimicrobial Peptide 99mTc-Ubiquicidin 29-41 as Human Infection-Imaging Agent: Clinical Trial. *J Nucl Med* **2005**, *46* (4), 567–573.

(58) Ebenhan, T.; Sathekge, M. M.; Lengana, T.; Koole, M.; Gheysens, O.; Govender, T.; Zeevaart, J. R. ^{68}Ga-NOTA-Functionalized Ubiquicidin: Cytotoxicity, Biodistribution, Radiation Dosimetry, and First-in-Human PET/CT Imaging of Infections. *J Nucl Med* **2018**, *59* (2), 334–339. https://doi.org/10.2967/jnumed.117.200048.

(59) Sathekge, M.; Garcia-Perez, O.; Paez, D.; El-Haj, N.; Kain-Godoy, T.; Lawal, I.; Estrada-Lobato, E. Molecular Imaging in Musculoskeletal Infections with 99mTc-UBI 29-41 SPECT/CT. *Ann Nucl Med* **2018**, *32* (1), 54–59. https://doi.org/10.1007/s12149-017-1219-7.

(60) Bhatt Mitra, J.; Chatterjee, S.; Kumar, A.; Bandyopadhyay, A.; Mukherjee, A. Integrating a Covalent Probe with Ubiquicidin Fragment Enables Effective Bacterial Infection Imaging. *RSC Med. Chem.* **2022**, *13* (10), 1239–1245. https://doi.org/10.1039/D2MD00190J.

(61) Welling, M. M.; Bunschoten, A.; Kuil, J.; Nelissen, R. G. H. H.; Beekman, F. J.; Buckle, T.; Van Leeuwen, F. W. B. Development of a Hybrid Tracer for SPECT and Optical Imaging of Bacterial Infections. *Bioconjugate Chem.* **2015**, *26* (5), 839–849. https://doi.org/10.1021/acs.bioconjchem.5b00062.

(62) Marjanovic-Painter, B.; Kleynhans, J.; Zeevaart, J. R.; Rohwer, E.; Ebenhan, T. A Decade of Ubiquicidin Development for PET Imaging of Infection: A Systematic Review. *Nuclear Medicine and Biology* **2023**, *116–117*, 108307. https://doi.org/10.1016/j.nucmedbio.2022.11.001.

(63) Golini, C. M.; Williams, B. W.; Foresman, J. B. Further Solvatochromic, Thermochromic, and Theoretical Studies on Nile Red. *Journal of Fluorescence* **1998**, *8* (4), 395–404. https://doi.org/10.1023/A:1020584801600.

(64) Martinez, V.; Henary, M. Nile Red and Nile Blue: Applications and Syntheses of Structural Analogues. *Chemistry A European J* **2016**, *22* (39), 13764–13782. https://doi.org/10.1002/chem.201601570.

(65) Karpenko, I. A.; Kreder, R.; Valencia, C.; Villa, P.; Mendre, C.; Mouillac, B.; Mély, Y.; Hibert, M.; Bonnet, D.; Klymchenko, A. S. Red Fluorescent Turn-On Ligands for Imaging and Quantifying G Protein-Coupled Receptors in Living Cells. *ChemBioChem* **2014**, *15* (3), 359–363. https://doi.org/10.1002/cbic.201300738.

(66) Hanser, F.; Marsol, C.; Valencia, C.; Villa, P.; Klymchenko, A. S.; Bonnet, D.; Karpenko, J. Nile Red-Based GPCR Ligands as Ultrasensitive Probes of the Local Lipid Microenvironment of the Receptor. *ACS Chem. Biol.* **2021**, *16* (4), 651–660. https://doi.org/10.1021/acschembio.0c00897.

(67) Sato, Y.; Kuwahara, K.; Mogami, K.; Takahashi, K.; Nishizawa, S. Amphipathic Helical Peptide-Based Fluorogenic Probes for a Marker-Free Analysis of Exosomes Based on Membrane-Curvature Sensing. *RSC Adv.* **2020**, *10* (63), 38323–38327. https://doi.org/10.1039/D0RA07763A.

(68) Mirloup, A.; Berthomé, Y.; Riché, S.; Wagner, P.; Hanser, F.; Laurent, A.; Iturrioz, X.; Llorens-Cortes, C.; Karpenko, J.; Bonnet, D. Alared: Solvatochromic and Fluorogenic Red Amino Acid for Ratiometric Live-cell Imaging of Bioactive Peptides. *Chemistry A European J* **2024**, e202401296. https://doi.org/10.1002/chem.202401296.

(69) Crader, M. F.; Kharsa, A.; Leslie, S. W. Bacteriuria. In *StatPearls*; StatPearls Publishing: Treasure Island (FL), 2024.

(70) Sharonov, A.; Hochstrasser, R. M. Wide-Field Subdiffraction Imaging by Accumulated Binding of Diffusing Probes. *Proc. Natl. Acad. Sci. U.S.A.* **2006**, *103* (50), 18911–18916. https://doi.org/10.1073/pnas.0609643104.

(71) Danylchuk, D. I.; Moon, S.; Xu, K.; Klymchenko, A. S. Switchable Solvatochromic Probes for Live-Cell Super-resolution Imaging of Plasma Membrane Organization. *Angew Chem Int Ed* **2019**, *58* (42), 14920–14924. https://doi.org/10.1002/anie.201907690.

(72) Manko, H.; Mély, Y.; Godet, J. Advancing Spectrally-Resolved Single Molecule Localization Microscopy with Deep Learning. *Small* **2023**, *19* (33), 2300728. https://doi.org/10.1002/smll.202300728.

(73) Zaritsky, A.; Woldringh, C. L. Chromosome Replication Rate and Cell Shape in Escherichia Coli: Lack of Coupling. *J Bacteriol* **1978**, *135* (2), 581–587. https://doi.org/10.1128/jb.135.2.581-587.1978.